EUROPEAN ORGANIZATION FOR NUCLEAR RESEARCH

LHWG Note 2001-2
ALEPH 2001-032 CONF 2001-024
DELPHI 2001-032 CONF 473
L3 Note 2656
OPAL Technical Note TN682
March 21, 2001
Updated March 26, 2001

Searches for the Neutral Higgs Bosons of the MSSM: Preliminary Combined Results Using LEP Data Collected at Energies up to 209 GeV

The ALEPH, DELPHI, L3 and OPAL Collaborations, and the LEP Higgs Working Group

Abstract

In the year 2000 the four LEP experiments collected data at centre-of-mass energies between 200 and 209 GeV, integrating approximately 870 pb^{-1} of luminosity, with about 510 pb^{-1} above 206 GeV. The LEP working group for Higgs boson searches has combined these data with data sets collected previously at lower energies. In representative scans of the parameters of the Minimal Supersymmetric Standard Model (MSSM), the mass limits $m_{\mathrm{h}} > 91.0$ GeV/c^2 and $m_{\mathrm{A}} > 91.9$ GeV/c^2 are obtained for the light CP-even and the CP-odd neutral Higgs boson, respectively. For a top quark mass less than or equal to 174.3 GeV/c^2, assuming that the stop quark mixing is maximal, and choosing conservative values for other SUSY parameters affecting the Higgs sector, the range $0.5 < \tan\beta < 2.4$ is excluded.

All results quoted in this note are preliminary.

1 Introduction

This note describes a combination of preliminary results of searches for the neutral Higgs bosons of the Minimal Supersymmetric Standard Model (MSSM) by the four LEP collaborations, ALEPH, DELPHI, L3 and OPAL. The results are based on data collected at $\sqrt{s} \approx 200 - 209$ GeV, the highest e^+e^- collision energies attained at LEP, and are combined with data collected earlier at lower centre-of-mass energies.

The MSSM predicts the existence of two complex scalar field doublets, with a total of eight degrees of freedom. As in the Standard Model (SM), three of the degrees of freedom appear as the longitudinal polarization states of the gauge bosons W^+, W^- and Z^0. The remaining five degrees of freedom are manifested in five physical scalar Higgs states. In this note, the Higgs sector of the MSSM is assumed to conserve CP. Under this assumption, the physical Higgs bosons are the CP-even h^0 and H^0, the CP-odd A^0, and the charged bosons H^+ and H^-. The quartic self-coupling of the Higgs fields are determined by the gauge couplings, which limits the mass of the lighter of the two CP-even Higgs bosons to be less than the mass of the Z^0 at tree level. Radiative corrections, particularly from loops containing the top quark, allow the lightest Higgs boson mass to range up to approximately 135 GeV/c^2, which is its maximal value [1] for all choices of parameters in the MSSM models within the constrained framework considered in this note (see Section 3.1). This constraint suggests that the lightest Higgs boson of the MSSM may be within the kinematic reach of searches at LEP. Searches are performed for the possible final states containing Higgs bosons and they are combined among the four collaborations in order to place the tightest constraints on the possible values of the MSSM Higgs sector.

In the MSSM, the Higgs-strahlung process $e^+e^- \to h^0Z^0$ proceeds as it does in the Standard Model, but its rate is suppressed by the factor $\sin^2(\beta - \alpha)$, where $\tan\beta$ is the ratio of the vacuum expectation values of the two field doublets, and α is the mixing angle in the neutral CP-even Higgs boson sector. The WW- and ZZ-fusion processes of the SM also proceed with a rate suppressed by the same factor relative to the SM rate. Heavy-Higgs-strahlung, $e^+e^- \to H^0Z^0$, occurs if it is kinematically possible, and has the SM production cross-section suppressed by the factor $\cos^2(\beta - \alpha)$. In some cases it can have a higher cross-section than $e^+e^- \to h^0Z^0$. The process $e^+e^- \to h^0A^0$ also occurs when kinematically allowed, and its production cross-section is proportional to $\cos^2(\beta - \alpha)$. Dedicated analyses are used to search for this final state.

The Higgs boson sector of the MSSM corresponds to a Type II two-Higgs-doublet model, in that the couplings of the Higgs fields to the fermions are constrained such that one Higgs field couples to the up-type fermions and the other to down-type fermions and charged leptons. This is arranged in order to avoid loop anomalies, to prevent flavour-changing neutral currents, and to give mass to the up-type and down-type fermions. This structure also implies that the decay branching ratios of the Higgs bosons to fermions depend not only on the masses, but also on the values of α and β. The coupling of the h^0 to $b\bar{b}$ is proportional to $-\sin\alpha/\cos\beta$; the coupling of the h^0 to $c\bar{c}$ is proportional to $\cos\alpha/\sin\beta$; the coupling of the A^0 to $b\bar{b}$ is proportional to $\tan\beta$; and the coupling of the A^0 to $c\bar{c}$ is proportional to $\cot\beta$. Over much of the parameter space considered, the h^0 and the A^0 decay predominantly into $b\bar{b}$ and $\tau^+\tau^-$ pairs, although for various choices of parameters, the decays $h^0 \to A^0A^0$, $h^0 \to c\bar{c}$, $h^0 \to gg$ and $h^0 \to W^+W^-$ can become important.

The searches that are combined in this note are the searches for the $e^+e^- \to h^0Z^0$ (and WW- and ZZ-fusion) processes which are used in the Standard Model interpretations

presented separately by the four collaborations in [2–5], combined with the searches for the $e^+e^-\to h^0A^0$ process described in [6–9]. In all combinations, a full specification of the production cross-sections at all relevant centre-of-mass energies and all decay branching ratios are incorporated into the calculations of the expected signal rates. The searches combined are sensitive predominantly to the $b\bar{b}$ and $\tau^+\tau^-$ decays of the h^0 and the A^0. A number of the abovementioned searches also have estimated efficiencies for the decays $h^0\to c\bar{c}$, gg, W^+W^-, A^0A^0 (with specified decays of the A^0, usually only to $b\bar{b}$), etc. The signal estimations for these searches also include the contributions from these sources. Specific flavour-blind searches for hadronically decaying Higgs bosons [9–11] are not yet included. The cross-sections and decay branching ratios are computed using HZHA03 [12], modified to use either the FeynHiggs calculations [1, 13] or SUBHPOLE2 [14].

Each experiment has generated Monte Carlo simulations of the signal processes and the SM background processes, typically at centre-of-mass energies of 200, 202, 204, 206, 208 and 210 GeV. The rates and distributions for energies in between the Monte Carlo points are interpolated.

The statistical procedure adopted for the combination of the data and the definitions of the confidence levels CL_s, CL_{s+b} and CL_b, are described in [15]. The main sources of systematic uncertainty in the estimations of the accepted signal and background rates are incorporated using an extension of the method of Cousins and Highland [16], where the correlations arising from shared error sources between analyses conducted at different energies, and between similar analyses conducted by the separate collaborations, are taken into account.

Searches for charged Higgs bosons are presented separately in [17].

2 Searches for $e^+e^-\to h^0A^0$

The analyses of the full data sample for the h^0Z^0 processes are documented in [2–5]. This section describes only the results of searches for $e^+e^-\to h^0A^0$. In the MSSM, $\cos^2(\beta-\alpha)$ is significantly different from zero only when $\tan\beta$ is large, which corresponds to points with $m_h \approx m_A$. Therefore the searches concentrate on the $b\bar{b}$ and $\tau^+\tau^-$ decays of the h^0 and the A^0. The numbers of selected events, the expected signal for m_h=90 GeV/c^2 and m_A=90 GeV/c^2, and the estimated background from SM processes are shown in Table 1, separately for each experiment. Also shown is the integrated luminosity reported by the experiments in the year 2000. Due to the β^3 kinematical factor dependence of the production cross-section for $e^+e^-\to h^0A^0$, the expected limits on the m_h=m_A diagonal are 10 GeV/c^2 below the highest energy recorded by LEP2 in 2000, and so the precise distribution of the beam energy is of less importance to the sensitivity of the h^0A^0 searches than it is to the h^0Z^0 searches.

3 Limits in the MSSM Parameter Space

The h^0Z^0 and A^0h^0 searches at LEP in the year 2000 are combined with previous LEP Higgs searches presented in [15] and references therein, conducted at centre-of-mass energies between $\sim$ 88 GeV and 202 GeV.

	ALEPH	DELPHI	L3	OPAL
$h^0A^0 \to b\bar{b}b\bar{b}$ channel				
Integrated Luminosity (pb^{-1})	217	224	217	208
Data	10	5	12	11
Total Background	5.5	6.5	7.8	10.3
Four-Fermion Bkg.	4.2	4.4	5.6	6.9
$q\bar{q}$ Background	1.4	2.1	2.2	3.4
Efficiency				
$m_h = m_A = 90$ GeV/c^2	47%	47%	42%	48%
Expected signal				
$m_h = m_A = 90$ GeV/c^2	3.5	3.6	3.2	3.4
$h^0A^0 \to b\bar{b}\tau^+\tau^-$ channel				
Integrated Luminosity (pb^{-1})	217	224	217	205
Data	3	5	2	5
Total Background	3.0	6.0	3.2	4.5
Four-Fermion Bkg.	2.8	5.6	2.9	4.1
$q\bar{q}$ Background	0.2	0.4	0.3	0.4
Efficiency				
$m_h = m_A = 90$ GeV/c^2	41%	25%	33%	43%
Expected signal				
$m_h = m_A = 90$ GeV/c^2	0.6	0.4	0.4	0.6
Limit obs (exp.med) for m_h (GeV/c^2)	89.6 (91.7)	89.8 (89.0)	83.7 (88.1)	79.3 (85.1)
Limit obs (exp.med) for m_A (GeV/c^2)	90.0 (92.1)	90.8 (90.0)	83.9 (88.3)	80.6 (86.9)

Table 1: The results in the A^0h^0 channels for each experiment for the data taken in 2000. Listed are the individual signal efficiencies, the expected signal counts, the total backgrounds, the backgrounds broken down into $q\bar{q}$ and four-fermion sources and the observed data counts, for each experiment's $h^0A^0 \to b\bar{b}b\bar{b}$ and $h^0A^0 \to b\bar{b}\tau^+\tau^-$ channel separately. The "tight selection" is shown for DELPHI's $h^0A^0 \to b\bar{b}b\bar{b}$ channel for easier comparison with the other experiments. The signal efficiencies and rates are given for $m_h = m_A = 90$ GeV/c^2, with $\tan\beta \sim 20$. Also listed are the observed and median expected lower bounds on m_h and m_A, taking the lower values of the limits obtained in the no-mixing and m_h−max scenarios. These scenarios are discussed in Section 3.

3.1 Benchmark Scenarios

We test for the presence of an MSSM Higgs boson signal using a constrained model with seven parameters, $M_{\rm SUSY}$, M_2, μ, A, $\tan\beta$, $m_{\rm A}$ and $m_{\tilde{\rm g}}$. All of the soft SUSY-breaking parameters in the sfermion sector are set to $M_{\rm SUSY}$ at the electroweak scale. M_2 is the SU(2) gaugino mass parameter at the electroweak scale, and M_1 is derived from M_2 using the GUT relation $M_1 = M_2(5\sin^2\theta_W/3\cos^2\theta_W)$, where θ_W is the weak mixing angle[1]. The supersymmetric Higgs boson mass parameter is denoted μ, and $\tan\beta$ is the ratio of the vacuum expectation values of the two Higgs field doublets. The parameter A is the common trilinear Higgs-squark coupling parameter, assumed to be the same for up-type squarks and for down-type squarks. The largest contributions to $m_{\rm h}$ from radiative corrections arise from stop loops, with much smaller contributions from sbottom loops. The gluino mass $m_{\tilde{\rm g}}$ affects loop corrections from both stops and sbottoms. The mass of the top quark is taken to be 174.3 GeV/c^2.

Three benchmark scenarios are considered [18]. The first ("no-mixing" scenario) assumes that there is no mixing between the scalar partners of the left-handed and the right-handed top quarks, with the following values and ranges for the parameters: $M_{\rm SUSY} = 1$ TeV/c^2, $M_2 = 200$ GeV/c^2, $\mu = -200$ GeV/c^2, $X_t(\equiv A - \mu\cot\beta) = 0$, $0.4 < \tan\beta < 50$ and 4 GeV/c^2 $< m_{\rm A} <$ 1 TeV/c^2. The gluino mass $m_{\tilde{\rm g}}$ is set to 800 GeV/c^2; it has little effect on the phenomenology of this scenario. Most of the experimental Monte Carlo samples assume that the $\rm h^0$ and $\rm A^0$ have decay widths which are small compared to the resolutions of the reconstructed masses; only DELPHI has performed tests in which the $\rm h^0$ and $\rm A^0$ widths are significant [7]. The assumption that the decay widths can be neglected is only valid for $\tan\beta < 30$ in this scenario, and hence higher values of $\tan\beta$ are not considered. The second scenario ("$m_{\rm h}$−max") is designed to yield the maximal value of $m_{\rm h}$ in the model. This scenario corresponds to the most conservative range of excluded $\tan\beta$ values. The same parameters are chosen as for the no-mixing scenario, except for the stop mixing parameter $X_t = 2M_{\rm SUSY}$ using the conventions of the two-loop diagrammatic calculation of [1]. Only values of $\tan\beta$ below 30 are considered in this model also in order to satisfy the assumptions made on the decay widths. The third scenario ("large μ" scenario) is a scan with parameters chosen to be $M_{\rm SUSY} = 400$ GeV/c^2, $\mu = 1$ TeV/c^2, $M_2 = 400$ GeV/c^2, $m_{\tilde{\rm g}} = 200$ GeV/c^2, $4 \le m_{\rm A} \le 400$ GeV/c^2, $X_t = -300$ GeV/c^2. This third scenario is designed to illustrate choices of MSSM parameters for which the Higgs boson $\rm h^0$ does not decay into pairs of b quarks due to cancellations from SUSY-QCD loops. This situation occurs at $\tan\beta > 20$ and for $120 < m_{\rm A} < 220$ GeV/c^2. The dominant decay modes of the $\rm h^0$ for these models are to $\rm c\bar{c}$ gg, $\rm W^+W^-$ and $\tau^+\tau^-$. For many of these models, the decay $\rm h^0 \to \tau^+\tau^-$ is also suppressed, providing an additional experimental challenge.

For all choices of parameters within the recommended ranges in the large μ scenario, the decay widths of the $\rm h^0$ and the $\rm A^0$ remain small when compared with the resolutions on the reconstructed masses. For this reason, the full recommended range of $\tan\beta$ up to 50 is considered in this scenario, in contrast to the first two scenarios.

For the no-mixing and $m_{\rm h}$−max scenarios, the two-loop diagrammatic approach of [1] is used to compute the relations between the SUSY parameters, $m_{\rm h}$, $m_{\rm A}$, $\tan\beta$, and the production cross-sections and decay branching ratios. For the large μ scenario, the one-loop renormalization-group improved calculation of [14, 19, 20] is used. These two

[1] M_3, M_2 and M_1 are the mass parameters associated with the SU(3), SU(2) and U(1) subgroups of the Standard Model. The relevance of M_3 only enters via loop corrections sensitive to the gluino mass.

calculations give consistent results [20], although small differences still exist. For example, in the $m_{\rm h}-$max scenario, the diagrammatic approach gives a more conservative upper edge of the excluded region of $\tan\beta$, while one-loop renormalization-group improved approach gives a slightly more conservative lower edge.

3.2 Results

The calculations of the confidence levels are performed for the three benchmark scenarios separately, and the results are shown in this section. The $m_{\rm h}-$max and no-mixing scenarios are described together in Section 3.2.1, while the large μ scenario is described separately in Section 3.2.2 because of qualitative differences in the features of these scenarios.

3.2.1 The $m_{\rm h}-$max and No-Mixing Scenarios

Figure 1 shows the $1-{\rm CL_b}$ significance contours as functions of $\rm h^0$ mass and $\rm A^0$ mass for the $m_{\rm h}-$max scenario. An excess is seen at $(m_{\rm h}, m_{\rm A}) \sim (83, 83)$ GeV/c^2, with a significance level slightly in excess of 2σ. This is due to candidates in the OPAL 189 GeV $\tau^+\tau^-{\rm b\bar{b}}$ channel [21] which have not been confirmed by later running or in other experiments; the significance has gradually decreased as additional luminosity has been accumulated. Another excess is seen near $(m_{\rm h}, m_{\rm A}) \sim (90, 90)$ GeV/c^2, due to candidates in the OPAL four-jet channel in the 196 GeV data [22], which also does not appear in other samples. The current 95% CL exclusion limits from LEP (shown also in the same figure) rule out both of these possibilities as an MSSM signal. In addition, due to the large range of models investigated and the fine reconstructed mass resolutions, the probability to have a 2σ excess somewhere is much larger than the 5% it would be if only a single counting experiment had been done. Over the range shown in Figure 1, the dilution factor of the significance is estimated to be 30–60. This estimation was performed by scaling the signal and background estimations of DELPHI and OPAL's test-mass-independent analyses of the 1999 and earlier data [2] by a factor of two, randomly generating candidates according to the background estimations, and for each set of random candidates, performing a confidence level calculation in the $m_{\rm h}$-max scenario and noting the smallest $1-{\rm CL_b}$ obtained. The probability of obtaining a particular value of $1-{\rm CL_b}$ or smaller was estimated and compared against $1-{\rm CL_b}$. More than one independent 2σ excess is probable.

A more detailed view of the combined $\rm e^+e^-\to h^0A^0$ search results is shown in Figure 2. Here, the values of $1-{\rm CL_b}$ and ${\rm CL_s}$ are shown for $m_{\rm h} \approx m_{\rm A}$ and at $\tan\beta$=20, as functions of $m_{\rm h}+m_{\rm A}$. For these models, $\cos^2(\beta-\alpha) \approx 1$, and the $\rm e^+e^-\to h^0Z^0$ searches do not contribute. The excesses mentioned above in the lower-energy data are seen in the plot of $1-{\rm CL_b}$. The quantity ${\rm CL_s}$ is used to exclude the signal hypothesis as a function of the MSSM parameters. The lowest unexcluded values of $m_{\rm h}$ and $m_{\rm A}$ correspond to models with lower values of $\tan\beta$, for which $m_{\rm A} \neq m_{\rm h}$, and so these lower bounds cannot be determined from Figure 2.

The 95% CL exclusion contours are shown in Figure 3 for the $m_{\rm h}-$max scenario, and in Figure 4 for the no-mixing scenario. The results for the large μ scenario are discussed separately below. In the no-mixing and $m_{\rm h}-$max scenarios, limits are shown

[2] Since this estimation was done, OPAL has created new test-mass-dependent analyses for the 1999 data.

in four projections: the ($m_{\rm h}$, $m_{\rm A}$) projection, the ($m_{\rm h}$, $\tan\beta$) projection, the ($m_{\rm A}$, $\tan\beta$) projection, and the ($m_{\rm H^{\pm}}$, $\tan\beta$) projection.

The observed and expected limits for $m_{\rm h}$ and $m_{\rm A}$ for the $m_{\rm h}-$max and no-mixing scenarios are given in Table 2. For the no-mixing scenario, the lower bounds on $m_{\rm h}$ and $m_{\rm A}$ are given for $\tan\beta > 0.76$ to highlight the search sensitivity to heavy Higgs bosons. For $\tan\beta < 0.76$, there is an unexcluded region with $m_{\rm A}$ below 40 GeV/c^2 and $m_{\rm h}$ above 65 GeV/c^2. This region is unexcluded because the $\rm e^+e^-\to h^0Z^0\to A^0A^0Z^0$ process dominates, and $\rm Br(A^0\to b\bar{b})$ is suppressed, either kinematically, when $m_{\rm A} < 10$ GeV/c^2, or because the coupling of the $\rm A^0$ to $\rm b\bar{b}$ becomes sufficiently suppressed so that exclusion via b-tagging channels becomes impossible. For unexcluded models in the no-mixing scenario with $\tan\beta < 0.76$, the mass of the charged Higgs boson is less than 74 GeV/c^2. The lower bound obtained by the combination of direct searches at LEP [17] is 78.5 GeV/c^2. The LEP charged Higgs boson searches assume however that $\rm Br(H^+\to c\bar{s})+Br(H^+\to\tau^+\nu_\tau)=1$. This assumption is broken by $\rm Br(H^+\to W^{*+}A^0)$, which can be as large as 0.6 for $\tan\beta = 0.76$ and $m_{\rm H^{\pm}}$=74 GeV/c^2, at the extremum of the unexcluded area. The decays of both the $\rm H^+$ and the $\rm H^-$ have to be considered in signal events. The LEP-combined limits on the cross-section assuming only fermionic $\rm H^{\pm}$ decays are of the order of 20% of the predicted cross-section for $m_{\rm H^{\pm}}$=74 GeV/c^2, and so it is not clear that the entire unexcluded region can be covered by the constraint from charged Higgs boson searches. Additional study is required to quantify the effect of the charged Higgs searches on this scenario.

For models with $m_{\rm A} < 4$ GeV/c^2, the decay branching fractions of the $\rm A^0$ are uncertain. In the $m_{\rm h}-$max scenario for all values of $m_{\rm h}$, and for the no-mixing scenario for $m_{\rm h} <$ 65 GeV/c^2, however, models with $m_{\rm A} < 4$ GeV/c^2 are excluded regardless of the $\rm A^0$ decay modes because the production cross-section for $\rm h^0Z^0$ multiplied by $\rm Br(h^0\to b\bar{b})$ provides a sufficient signal to exclude these models.

Scenario	$m_{\rm h}$ limit (GeV/c^2) $\tan\beta > 1.2$	$m_{\rm A}$ limit (GeV/c^2) $\tan\beta > 1.2$	Excluded $\tan\beta$ observed limit (expected limit)
$m_{\rm h}-$max	91.0 (94.6)	91.9 (95.0)	$0.5 < \tan\beta < 2.4$ ($0.5 < \tan\beta < 2.6$)
No Mixing	91.5 (95.0)	92.2 (95.3)	$0.8 < \tan\beta < 9.6$ ($0.8 < \tan\beta < 16.8$)

Table 2: Limits on $m_{\rm h}$ and $m_{\rm A}$ in the $m_{\rm h}-$max and no-mixing benchmark scenarios explained in the text. The median expected limits in an ensemble of SM background-only experiments are listed in parentheses. To highlight the sensitivity of the searches for massive Higgs bosons, the limits on $m_{\rm h}$ and $m_{\rm A}$ are given with the additional constraint of $\tan\beta > 0.76$ for the no-mixing scenario. If $\tan\beta$ is explored in the full region to 0.4, then values of $m_{\rm A}$ below 40 GeV/c^2 are not excluded for values of $m_{\rm h}$ above 65 GeV/c^2 in the no-mixing scenario. The excluded regions for all three scenarios are shown in Figures 3, 4 and 5.

The searches presented here allow regions of $\tan\beta$ to be excluded within the contexts of the $m_{\rm h}-$max and no-mixing scenarios. For the $m_{\rm h}-$max scenario, values of $\tan\beta$ between 0.5 and 2.4 are excluded, while for the no mixing scenario, values of $\tan\beta$ between 0.8 and 9.6 are excluded. The $\tan\beta$ limits in the $m_{\rm h}-$max scenario are determined by the exclusion limit for the $\rm h^0Z^0$ process, which depends strongly on the centre-of-mass energies LEP achieved. For the no-mixing scenario, the $\tan\beta$ limits are more complex. The maximum value of $m_{\rm h}$ in the no mixing scenario is approximately 114 GeV/c^2, and occurs

when $m_{\rm A}$ is large (the SM-like limit). The expected SM mass limit is 115.3 GeV/c^2 [24], and the only models in this scan which are expected to be unexcluded (aside from the low-tan β models mentioned above) have $m_{\rm h} \approx m_{\rm A}$, with $m_{\rm h} + m_{\rm A} > \sqrt{s}$. The extent of this region in model space is determined by the sensitivity of the $\rm h^0A^0$ searches, and determines the expected upper edge of the excluded region of tan β. On the other hand, the observed SM limit of 113.5 GeV/c^2 leaves unexcluded some models with large $m_{\rm A}$, and the observed tan β limit in the no-mixing scenario is determined by the candidates in the $\rm h^0Z^0$ searches.

In a more general scan, where the MSSM parameters are varied independently and the top quark mass is allowed to be as large as 185 GeV, the limits on $m_{\rm h}$, $m_{\rm A}$ and tan β are weaker (see the discussions of Ref. [21]). In particular, if the mass of the top quark is 179 GeV/c^2 (higher by 1σ than the measured central value), then tan β can no longer be excluded above 1.9 or below 0.6 in the $m_{\rm h}-$max scenario.

3.2.2 The Large μ Scenario

The excluded models in the large μ scenario are shown in Figure 5. For this scenario, only the ($m_{\rm A}$, tan β) projection is shown because all of the unexcluded points have $m_{\rm h} \approx$ 107 GeV/c^2, close to the maximum possible $m_{\rm h}$ in this scenario. The unexcluded model points are kinematically within reach of the LEP experiments but signal events would not be detected because the leading decay branching ratios of the $\rm h^0$ are to $\rm c\bar{c}$, gluons and $\rm W^+W^-$; the $\rm b\bar{b}$ decays are suppressed by the choice of model parameters and there is an insufficient branching ratio of the $\rm h^0$ to $\tau^+\tau^-$. While some of the searches which are included have some efficiency for the non-$\rm b\bar{b}$ and non-$\tau^+\tau^-$ decays of the $\rm h^0$, the flavour-independent searches of the LEP collaborations [9–11] are not included in the combinations presented here[3]. Further work to include these will be useful in order to study the large μ scenario.

An additional feature of the large μ scenario is the presence of models for which the production, via Higgs-strahlung, of the heavy Higgs boson $\rm H^0$ is kinematically possible. For some choices of the model parameters, $m_{\rm h} \approx m_{\rm A}$, $\cos^2(\beta-\alpha) \approx 1$ and $m_{\rm h}+m_{\rm A} > \sqrt{s}$. For these cases, the production of $\rm h^0Z^0$ is suppressed by the small value of $\sin^2(\beta-\alpha)$, and the production of $\rm h^0A^0$ is not allowed by the kinematics. In this scenario for these parameters, the heavy Higgs boson is light enough to allow the searches for $\rm h^0Z^0$ to be reinterpreted as searches for $\rm H^0Z^0$, using the complete calculation of the $\rm H^0Z^0$ production cross-section (proportional to $\cos^2(\beta-\alpha)$), and decay branching ratios. This switch of interpretation is done if $\sigma_{\rm h^0Z^0} \times {\rm Br}({\rm h^0}\to{\rm b\bar{b}}) < \sigma_{\rm H^0Z^0} \times {\rm Br}({\rm H^0}\to{\rm b\bar{b}})$ at $\sqrt{s} = 202$ GeV. The smaller signal for $\rm h^0Z^0$ is then ignored in the confidence level calculation. In the $m_{\rm h}-$max and no-mixing scenarios, the heavy Higgs boson is usually out of kinematic reach and this interpretation is not done.

References

[1] S. Heinemeyer, W. Hollik and G. Weiglein, Phys. Rev. **D58** (1998) 091701, Eur. Phys. J. **C9** (1999) 343, Phys. Lett. **B440** (1998) 296, hep-ph/9807423 and JHEP 0006

[3]The flavour-independent searches have overlaps in their signal and background expectations with the b-tagging analyses, and select some of the same events in the data. Additional work is needed to combine these properly for all experiments

(2000) 009.

[2] ALEPH Collab., R. Barate *et al.*, "Observation of an excess in the search for the Standard Model Higgs boson at ALEPH", CERN-EP/2000-138, published in Phys. Lett. **B495** (2000) 1.

[3] DELPHI Collab., P. Abreu *et al.*, "Search for the Standard Model Higgs boson at LEP in the year 2000", CERN-EP-2001-004, published in Phys. Lett. **B499** (2001) 23.

[4] L3 Collab., M. Acciari *et al.*, "Higgs candidates in e^+e^- interactions at $\sqrt{s} = 206.6$ GeV, CERN-EP-2000-140, published in Phys. Lett. **B495** (2000) 18.

[5] OPAL Collab., "Search for the Standard Model Higgs Boson in e^+e^- Collisions at $\sqrt{s} \approx 192 - 209$ GeV", CERN-EP-2000-156, published in Phys. Lett. **B499** (2001) 38.

[6] ALEPH Collab., "Searches for neutral Higgs bosons of the MSSM at centre-of-mass energies up to 209 GeV with teh ALEPH detector at LEP", ALEPH 2001-022 CONF 2001-019, 6 March, 2001.

[7] DELPHI Collab., "Searches for neutral supersymmetric Higgs bosons in e^+e^- collisions up to $\sqrt{s} = 209$ GeV", DELPHI 2001-017 CONF 458, 7 March, 2001.

[8] A. Raspereza, L3 Collaboration, "Searches for Higgs bosons beyond the SM with the L3 detector", presentation given at Higgs and Supersymmetry, Orsay, 19–22 March, 2001.

[9] OPAL Collab., "Searches for Higgs Bosons in Extensions to the Standard Model in e^+e^- Collisoins at the Highest LEP Energies" OPAL Physics Note PN472, 27 February, 2001.

[10] ALEPH Collab., "A flavour-independent search for the Higgsstrahlung process in e^+e^- collisions at centre-of-mass energies from 189 to 209 GeV", ALEPH 2001-021 CONF 2001-018.

[11] L3 Collab., "Search for Production of Neutral Higgs Scalars in e^+e^- Annihilations at LEP", L3 Note 2576, 7 July, 2000.

[12] HZHA generator: P. Janot, in "Physics at LEP2", edited by G. Altarelli, T. Sjöstrand and F. Zwirner, CERN 96-01 Vol. 2 p.309.
For HZHA3 and HZHA2, see `http://alephwww.cern.ch/~janot/Generators.html`.

[13] S. Heinemeyer, W. Hollik and G. Weiglein, Comp. Phys. Comm. **124** (2000) 76; Also see `http://www.feynhiggs.de`.

[14] M. Carena, M. Quirós and C.E.M. Wagner, Nucl. Phys. **B461** (1996) 407, hep-ph/9508343.

[15] ALEPH, DELPHI, L3, OPAL Collab., and the LEP working group for the Higgs boson searches, "Search for Higgs bosons: Preliminary combined results using LEP data collected at energies up to 202 GeV," CERN-EP/2000-055, 25 Apr 2000.

[16] R. D. Cousins and V. L. Highland, Nucl. Instr. Meth **A320** (1992) 331.

[17] ALEPH, DELPHI, L3 and OPAL Collaborations, and the LEP Higgs Working Group, "Search for Charged Higgs boson: Preliminary combined results using LEP data collected at energies up to 209 GeV" LEP Higgs WG note 2001-1, L3 Note 2653, OPAL Technical Note TN680.

[18] M. Carena, S. Heinemeyer, C. E. M. Wagner and G. Weiglein, hep-ph/9912223.

[19] M. Carena, S. Mrenna and C. Wagner, Phys. Rev. D60 (1999) 075010.

[20] M. Carena, H. E. Haber, S. Heinemeyer, W. Hollik, C. E. M. Wagner and G. Weiglein, " Reconciling the Two-Loop Diagrammatic and Effective Field Theory Computations of the Mass of the lightest CP-even Higgs Boson in the MSSM", Nucl. Phys. **B580** (2000) 29.

[21] OPAL Collab., G. Abbiendi *et al.*, Eur. Phys. J. **C12** (2000) 567-586.

[22] OPAL Collab., "Search for Neutral Higgs Bosons in e^+e^- Collisions at $\sqrt{s} \approx 192 - 202$ GeV", OPAL Physics Note PN426, 3 Mar 2000.

[23] A. G. Akeroyd and W. J. Stirling, Nucl. Phys. **B447** (1995), 3.

[24] P. Igo-Kemenes, "Status of Higgs Boson Searches", November 3, 2000, LEPC presentation, http://lephiggs.web.cern.ch/LEPHIGGS/talks/index.html.

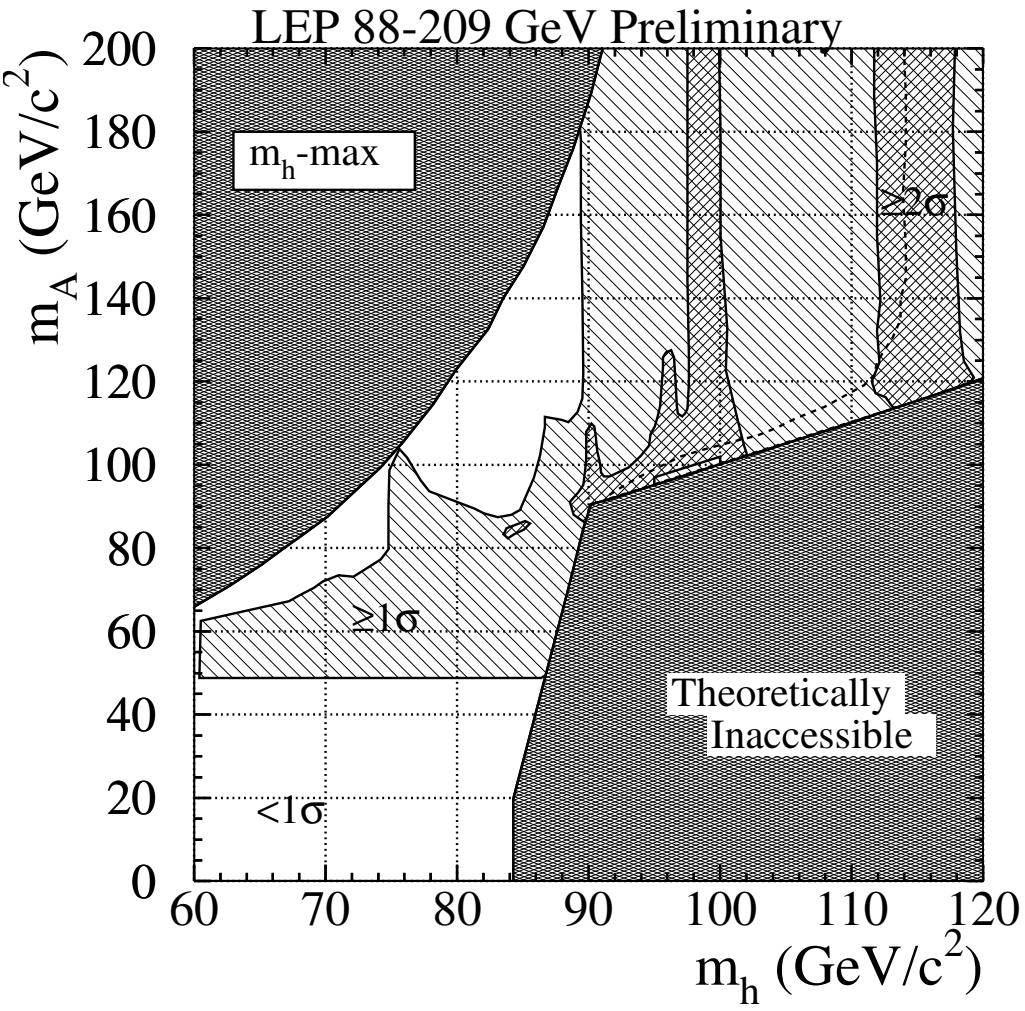

Figure 1: The distribution of the confidence level CL_b in the (m_h, m_A) plane for the m_h-max scenario. In the white domain, the observation either shows a deficit or is less than 1σ above the background prediction, while in the domains labelled $\geq 1\sigma$ and $\geq 2\sigma$, the observation shows an excess above the SM background prediction by the indicated amount. If at a point (m_h, m_A) in the plane, two values of $\tan\beta$ are allowed by the benchmark model, the choice of $\tan\beta$ with the larger CL_b is shown. Results from the h^0Z^0 searches are combined with the results of the A^0h^0 searches. Vertical structures are due to features in the h^0Z^0 search results, while structure on the m_h=m_A line arises from the A^0h^0 searches. The 95% CL exclusion contour is shown with the dashed line; points to the right and below the dashed line are unexcluded. These regions can also be seen in Figure 3.

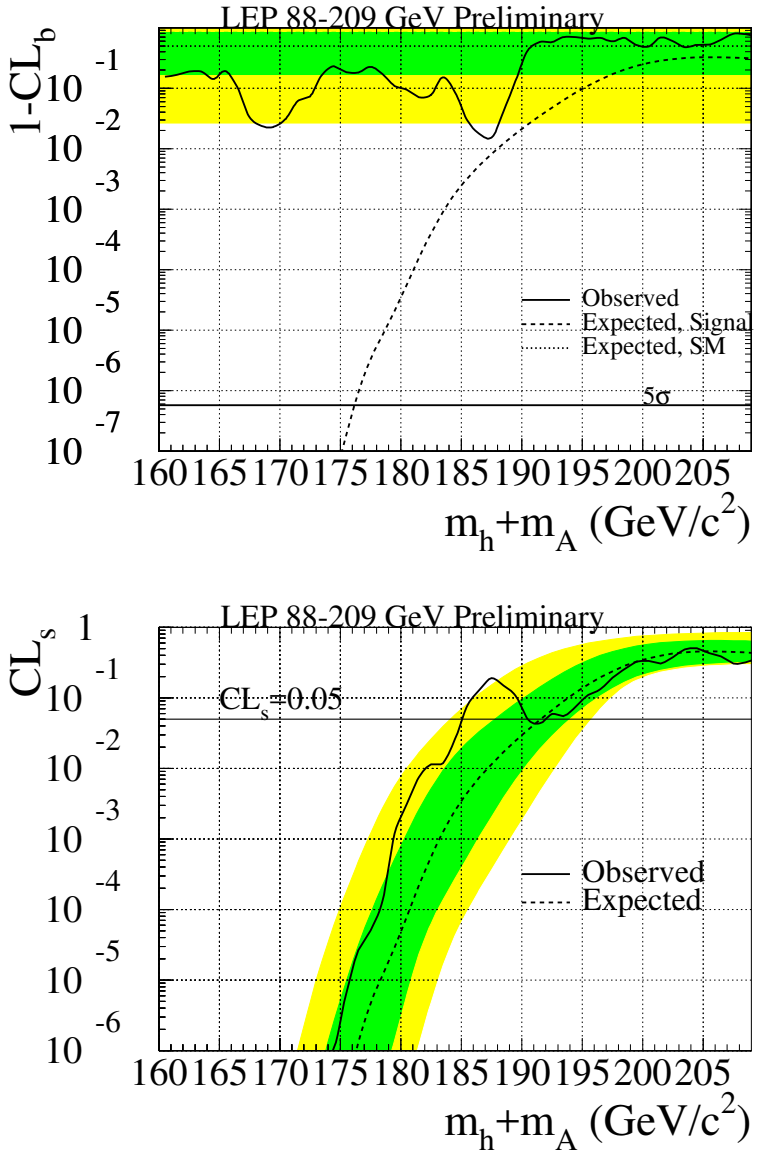

Figure 2: The values of $1 - \mathrm{CL_b}$ and $\mathrm{CL_s}$ for the $m_\mathrm{h} \approx m_\mathrm{A}$ diagonal ($\tan\beta > 20$, $\cos^2(\beta - \alpha) \approx 1$) in the $m_\mathrm{h}-$max scenario. The top plot shows the observed value of $1 - \mathrm{CL_b}$ as a function of $m_\mathrm{h} + m_\mathrm{A}$ in this scenario, as well as its median expected value (dashed line) in the presence of a signal at the test mass. The value of $1-\mathrm{CL_b}$ is expected to be uniformly distributed between zero and one if there is no signal present. The dark shaded band is the 68% probability region centred on $1-\mathrm{CL_b} = 0.5$, and the light-shaded band is the 95% probability region centred also on $1 - \mathrm{CL_b} = 0.5$. The solid line labelled "5σ" is drawn at $1 - \mathrm{CL_b} = 5.7 \times 10^{-7}$. In the lower plot, the observed value of $\mathrm{CL_s}$ is shown in the same scenario for the same high-$\tan\beta$ models. The median expected $\mathrm{CL_s}$ in an ensemble of background-only experiments is shown with a dashed line, and 68% and 95% probability contours are shown with dark and light shading, respectively. Models with $\mathrm{CL_s} < 0.05$ are excluded at the 95% confidence level. The lowest unexcluded values of m_h and m_A correspond to models with lower values of $\tan\beta$, for which $m_\mathrm{A} \neq m_\mathrm{h}$.

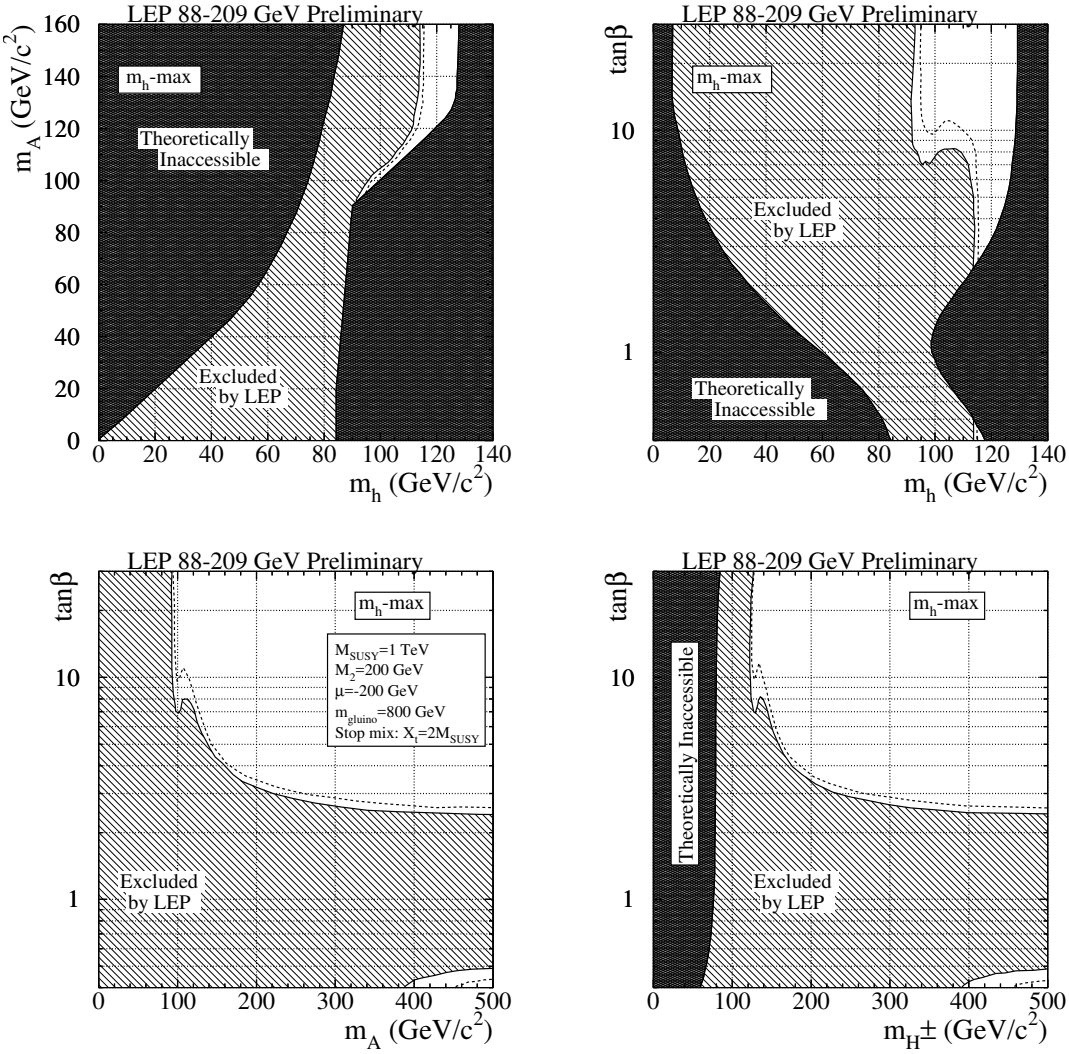

Figure 3: The MSSM exclusion for the $m_{\mathrm{h}}-$max benchmark scenario described in the text of Section 3. This figure shows the excluded (diagonally hatched) and theoretically disallowed (cross-hatched) regions as functions of the MSSM parameters in four projections: (upper left) the (m_{h}, m_{A}) plane, (upper right) the (m_{h}, $\tan\beta$) plane, (lower left) the (m_{A}, $\tan\beta$) plane and (lower right) the ($m_{\mathrm{H}^{\pm}}$, $\tan\beta$) plane. The dashed lines indicate the boundaries of the regions expected to be excluded at the 95% CL if only SM background processes are present.

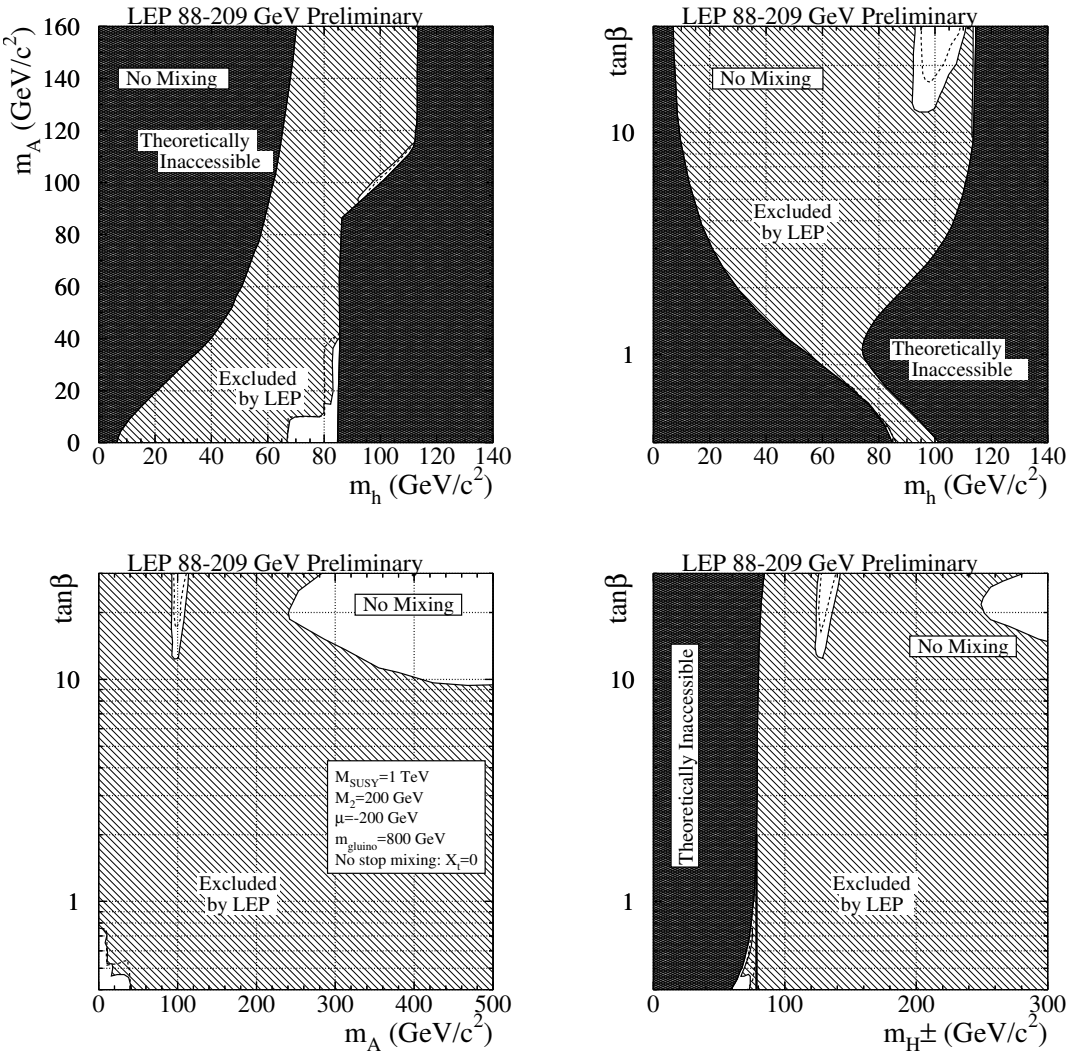

Figure 4: The MSSM exclusion for the "no mixing" benchmark scenario described in the text of Section 3. This figure shows the excluded (diagonally hatched) and theoretically inaccessible (cross-hatched) regions as functions of the MSSM parameters in four projections: (upper left) the ($m_{\rm h}$, $m_{\rm A}$) plane, (upper right) the ($m_{\rm h}$, $\tan\beta$) plane, (lower left) the ($m_{\rm A}$, $\tan\beta$) plane and (lower right) the ($m_{\rm H^\pm}$, $\tan\beta$) plane. The dashed lines indicate the boundaries of the regions expected to be excluded at the 95% CL if only SM background processes are present. In the ($m_{\rm H^\pm}$, $\tan\beta$) projection, a dark vertical line is drawn at $m_{\rm H^\pm}$=78.5 GeV/c^2, the lower bound obtained from direct searches at LEP. Due to the decays $\rm H^\pm \to W^{*\pm} A^0$, however, models with $m_{\rm H^\pm} < 74$ may not be excluded by the direct searches. More study is needed to make a quantitative estimation of the impact of the $\rm H^\pm$ searches on this scenario.

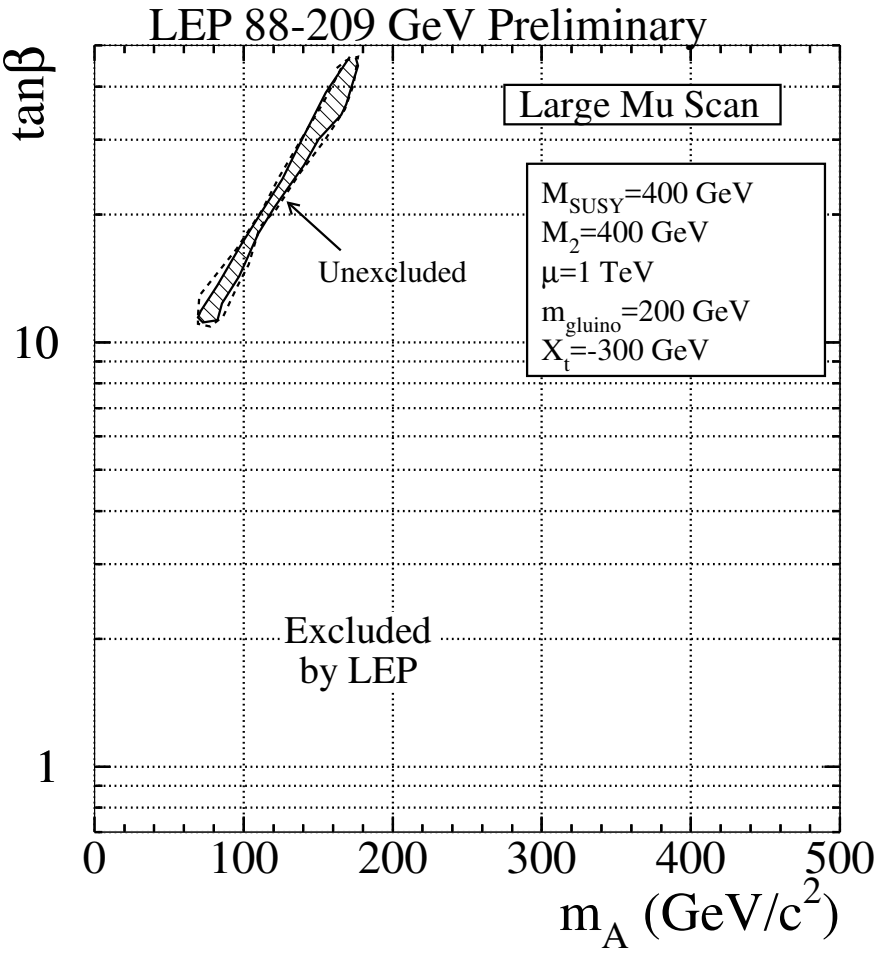

Figure 5: The MSSM exclusion for the "large μ" benchmark scenario described in the text of Section 3. This figure shows the unexcluded region as diagoanlly hatched in the (m_{A}, $\tan\beta$) plane. Models with $\tan\beta < 0.7$ are not investigated because of the instability of the numerical calculations [14]. Only the (m_{A}, $\tan\beta$) projection is shown because all of the unexcluded models have $m_{\mathrm{h}} \approx 107$ GeV/c^2.